



Synthesis and antiproliferative evaluation of pyrazolo[1,5-*a*]-1,3,5-triazine myoseverin derivatives

Florence Popowycz^a, Cédric Schneider^a, Salvatore DeBonis^b, Dimitrios A. Skoufias^b, Frank Kozielski^c, Carlos M. Galmarini^d, Benoît Joseph^{a,*}

^a Institut de Chimie et Biochimie Moléculaires et Supramoléculaires, UMR–CNRS 5246, Université de Lyon, Université Claude Bernard–Lyon 1, Bâtiment Curien, 43 Boulevard du 11 Novembre 1918, F-69622 Villeurbanne, France

^b Institut de Biologie Structurale (CEA-CNRS-UJF), 41 rue Jules Horowitz, 38027 Grenoble Cedex 01, France

^c The Beatson Institute for Cancer Research, Switchback Road, Bearsden, G61 1BD Glasgow, UK

^d ENS-CNRS UMR 5239, UFR de Médecine Lyon-Sud, 165 chemin du Grand Revoyet, BP 12, 69921 Oullins, France

ARTICLE INFO

Article history:

Received 12 November 2008

Revised 2 March 2009

Accepted 3 March 2009

Available online 10 March 2009

Keywords:

Myoseverin

Pyrazolo[1,5-*a*]-1,3,5-triazine

Tubulin

Cancer

ABSTRACT

Pyrazolo[1,5-*a*]-1,3,5-triazine myoseverin derivatives **1a–c** were prepared from 4-(*N*-methyl-*N*-phenylamino)-2-methylsulfanylpyrazolo[1,5-*a*]-1,3,5-triazine **2**. Their cytotoxic activity, inhibition of tubulin polymerization, and cell cycle effects were evaluated. Compounds **1a** and **1c** are potent tubulin inhibitors and displayed specific antiproliferative activity in colorectal cancer cell lines at micromolar concentrations.

© 2009 Elsevier Ltd. All rights reserved.

1. Introduction

Myoseverin (Fig. 1) has been initially identified as a new microtubule assembly inhibitor with moderate cytostatic activity from a library of 2,6,9-trisubstituted purines.¹ The same compound was shown to convert multinucleated myotubes to proliferative myoblast-like cells by disrupting microtubule assembly.^{1a,2} Recently, myoseverin was also described as a potential inhibitor of new vessel growth by inhibiting endothelial cell function and differentiation of progenitor cells.³ Further optimization of myoseverin led to the preparation of two new myoseverin derivatives,^{1b,4} 8-azamyoseverin and pyrazolo[4,3-*d*]pyrimidine (E2GG) analogues that contain similar structural motifs (Fig. 1).⁵ E2GG displayed higher antiproliferative activity compared to myoseverin in several human cancer cell lines. Trisubstituted 1,3,5-triazine derivatives⁶ such as tubulizyne were also designed with potent microtubule disassembly properties.

According to the literature,⁷ the purine nucleus and the pyrazolo[1,5-*a*]-1,3,5-triazine ring are structurally close and possess strikingly similar biophysicochemical properties (electrostatic potential surface, isopotential curve, charges). Improved metabolic stability was also observed for the pyrazolo[1,5-*a*]-1,3,5-triazine

P2Y1 receptor antagonist compared to the purine analogue.⁸ In our group, we recently reported the design of pyrazolo[1,5-*a*]-1,3,5-triazine (*R*)-roscovitine bioisostere which displayed significantly higher biological potency compared to purine (*R*)-roscovitine.⁹

In this article, we investigated the synthesis of novel pyrazolo[1,5-*a*]-1,3,5-triazine myoseverin-like molecules **1a–c** (Fig. 1) in order to compare their antiproliferative and tubulin inhibitory activities with those obtained for myoseverin.

2. Chemistry

The synthesis of 2,4,8-trisubstituted pyrazolo[1,5-*a*]-1,3,5-triazines **1a–c** is reported in Schemes 1 and 2. The starting material 4-(*N*-methyl-*N*-phenylamino)-2-(methylsulfanyl)pyrazolo[1,5-*a*]-1,3,5-triazine **2**¹⁰ was oxidized by *m*-CPBA to afford the sulfonyl derivative **3** in fair yield (78%). Nucleophilic aromatic substitution was performed in the presence of **3** and 4-methoxybenzylamine in excess in dioxane at 140 °C for 24 h (sealed tube). The final compound **1a** was obtained in 70% yield. The derivative **1b** was also prepared from **2**. Bromination of **2** occurred regioselectively on the C-8 position (NBS, CHCl₃) to afford **4** in 82% yield. Oxidation of **4** (84% yield), followed by a double addition–elimination reaction on **5** in the presence of 4-methoxybenzylamine gave **1b** in 70% yield. For the preparation of **1c**, the alkyl chain was first

* Corresponding author. Tel.: +33 (0)4 72 44 81 35; fax: +33 (0)4 72 43 12 14.
E-mail address: benoit.joseph@univ-lyon1.fr (B. Joseph).

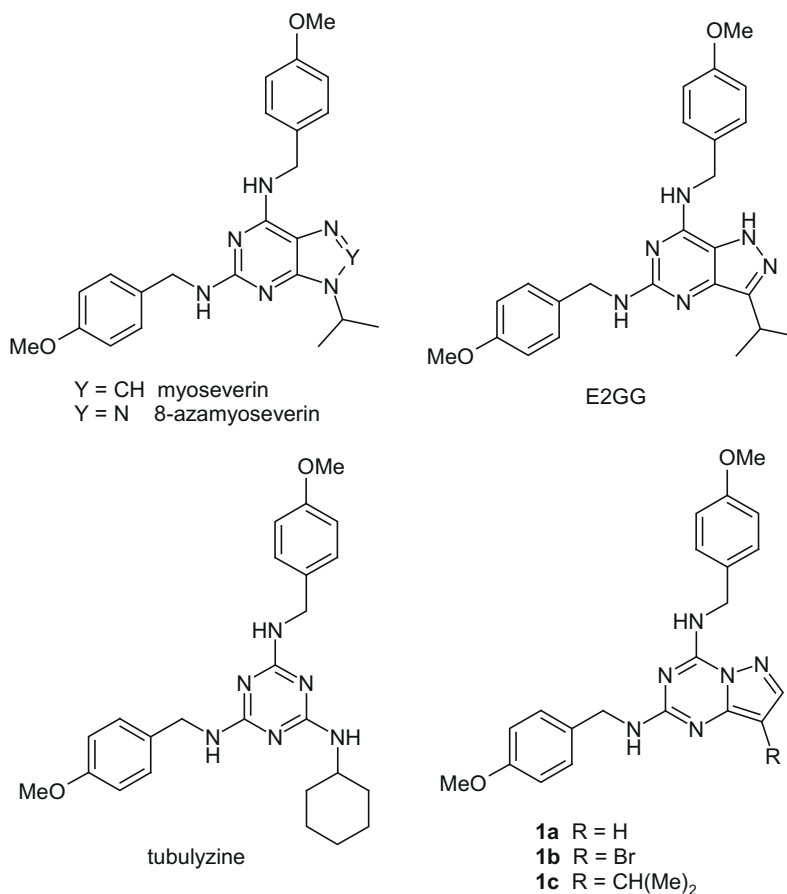
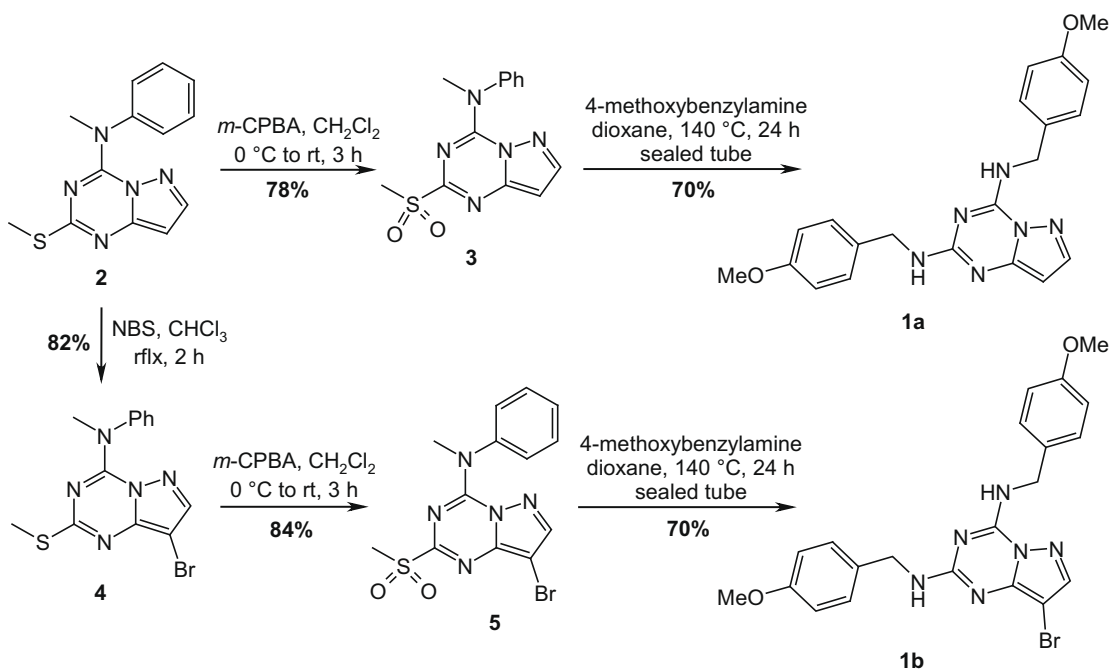


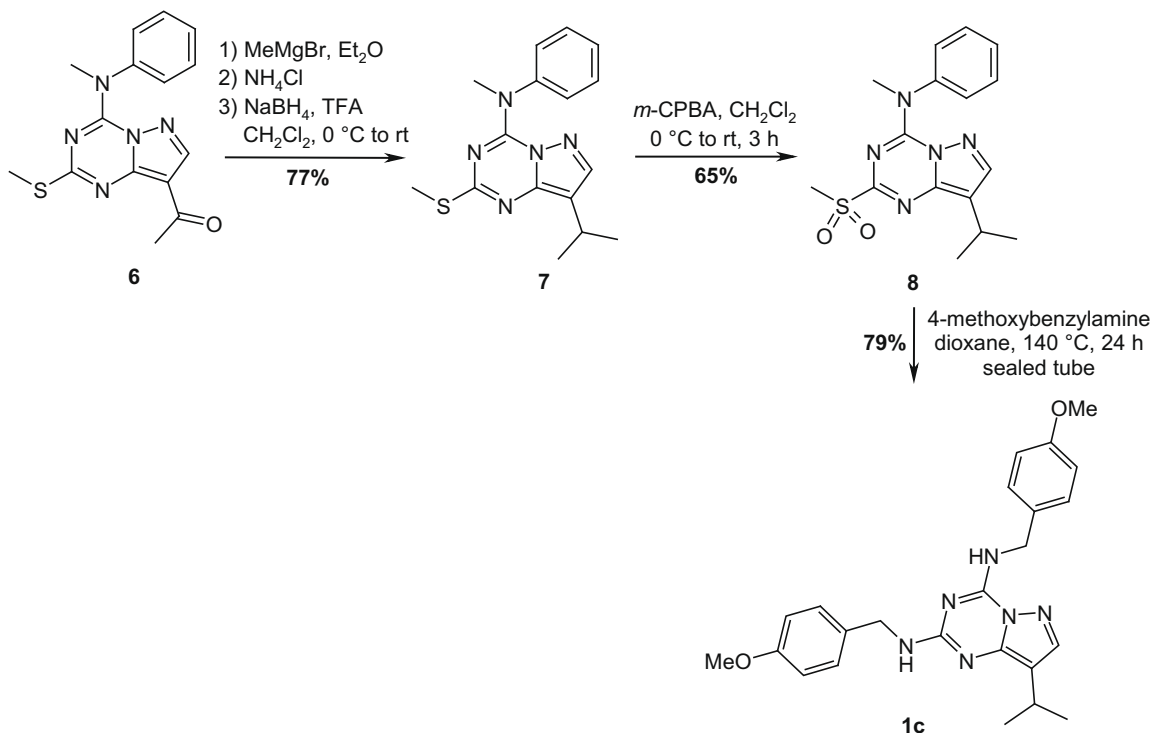
Figure 1. Chemical structures of myoseverin, 8-azamyoseverin, E2GG, tubulyzine and 1a–c.

built-up on the pyrazolo[1,5-*a*]-1,3,5-triazine moiety. The 8-acetyl-4-(*N*-methyl-*N*-phenylamino)-2-(methylsulfanyl)pyrazolo[1,5-*a*]-1,3,5-triazine **6**¹⁰ was treated with methylmagnesium bromide,

then the magnesium complex was smoothly hydrolyzed with NH₄Cl. Without further purification, the crude tertiary alcohol was submitted to a dehydroxylation reaction in a NaBH₄/TFA mix-



Scheme 1.



Scheme 2.

ture in CH_2Cl_2 to afford **7** in 77% two step yield. As reported for **1a** and **1b**, oxidation of **7** (65% yield) followed by the $\text{S}_\text{N}\text{Ar}$ reaction on **8** afforded **1c** in good yield.

3. Results and discussion

3.1. Growth inhibitory effects of myoseverin, **1a**, **1b** and **1c**

Cell growth inhibition of myoseverin and pyrazolo[1,5-*a*]-1,3,5-triazine derivatives **1a–c** was evaluated using different cancer cell lines. As shown in Table 1, myoseverin was active at low μM ranges (2.7–11.5 μM) in all the tested cell lines being most active in the colorectal cancer cell lines (HCT116, SW48 and SW480). Compound **1c** displayed a higher antiproliferative activity in colorectal cancer cell lines and in CEM cells. The cell growth inhibition activity of **1c** observed in these cell lines was similar to that observed after myoseverin treatment. In contrast, the MCF-7 and the Mes-sa cells responded only marginally to this compound at concentrations higher than 20 μM . A similar antiproliferative pattern was observed after treatment of the cell lines with **1a**. However, this compound was less active than **1c** and myoseverin in the CEM cells. Finally, **1b** displayed some antiproliferative activity only towards the SW48 cells. In the other cell lines, the compound showed IC_{50} values higher than 20 μM .

3.2. Cell cycle analysis

To characterize the effects of pyrazolo[1,5-*a*]-1,3,5-triazine derivatives on the cell cycle, proliferating colorectal cancer cell lines (HCT116, SW48 and SW480) were treated with **1a**, **1b**, **1c** and myoseverin at 30 μM and analyzed by flow cytometry (Table 2). Myoseverin was found to arrest the cell cycle at the G_2/M phases in the three analyzed cell lines. Similarly, by 24 h of treatment with **1c**, a substantial number of cells were arrested at G_2/M phases at levels similar to those observed for myoseverin. In contrast, **1a** and **1b** that presented a lower antiproliferative activity than myoseverin in these cell lines, also showed a lower amount of cells blocked at G_2/M phases.

3.3. Microtubule polymerization assays

The three pyrazolo[1,5-*a*]-1,3,5-triazine derivatives and myoseverin as control were tested in microtubule polymerization assays using bovine brain purified tubulin (Table 3). The IC_{50} for myoseverin is 3.6 μM in good agreement with previous results that found an IC_{50} value of 7–8 μM .^{1b,5} Both **1c** (Fig. 2) and **1a** are equally potent effectors of microtubule polymerization than myoseverin with IC_{50} values of 3.6 and 3.4 μM , respectively. They both reduced the rate and the final extent of microtubule assembly. Fifty

Table 1
In vitro cell growth inhibition activities of myoseverin and **1a–c** in human cancer cell lines

Compound	$\text{IC}_{50}^{\text{a,b}}$ (μM)					
	MCF-7	Mes-sa	CEM	HCT116	SW48	SW480
Myoseverin	11.5 ± 0.7	8.5 ± 0.7	5.7 ± 0.3	3.3 ± 0.1	2.7 ± 0.4	4.8 ± 1.6
1a	34 ± 8	45 ± 7	13 ± 7	6.2 ± 1	5.2 ± 0.3	8.1 ± 2.3
1b	35.5 ± 4.9	43 ± 1.4	38.5 ± 9	25 ± 4.2	7.5 ± 0.7	26.5 ± 2.1
1c	51.5 ± 4.9	23 ± 2.4	5.4 ± 0.5	4.6 ± 3	2.6 ± 0.2	5.5 ± 0.9

^a Values are means of three different experiments ± SD.

^b IC_{50} : Inhibitory concentration 50.

Table 2
Percentage of cells (%) in different phases of the cell cycle

Compound ^a	HCT116			SW48			SW480		
	G ₁ ^b	S	G ₂ /M	G ₁	S	G ₂ /M	G ₁	S	G ₂ /M
Control	62.5 ± 11.5	26.1 ± 9.7	11.3 ± 4.4	60.5 ± 3.6	23.3 ± 5.5	16.1 ± 8.8	57.6 ± 6.9	28.7 ± 5	13.6 ± 4.5
Myoseverin	1.8 ± 0.3	9.5 ± 3.5	88 ± 4.2	1 ± 1.4	1 ± 0	98 ± 1.4	12.5 ± 0.8	3 ± 1.4	84.5 ± 2
1a	19 ± 2.8	29 ± 1.4	51 ± 4.2	16 ± 4.2	21 ± 5.7	62 ± 9.9	43 ± 1.4	15 ± 1.4	42 ± 2.8
1b	44 ± 2.8	0.5 ± 0.7	55.5 ± 2.1	50 ± 9.9	0.5 ± 0.7	42.5 ± 0.7	62 ± 2.8	9 ± 1.4	28 ± 5.7
1c	8 ± 1.5	2.8 ± 2.5	89.3 ± 1	22.4 ± 5.3	1.3 ± 0.4	75.4 ± 4.7	3 ± 0.2	5.9 ± 0.8	91.2 ± 0.7

^a Compounds were tested at 30 μM.

^b Values are means of three different experiments ± SD.

Table 3
In vitro inhibition of bovine brain purified tubulin polymerization of myoseverin and **1a–c**

Compound	IC ₅₀ (μM)
Myoseverin	3.6
1a	3.4
1b	50% Baseline
1c	3.6

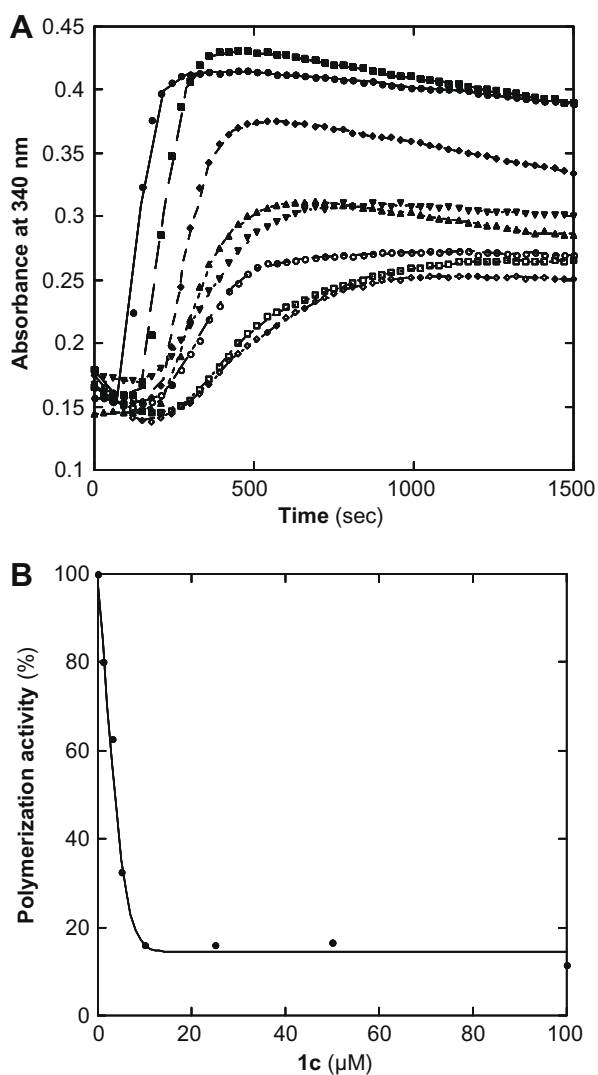


Figure 2. (A) In vitro inhibition of tubulin assembly for **1c** measured at a protein concentration of 29 μM and increasing inhibitor concentrations up to 100 μM. (B) Concentration–response plot for compound **1c**, derived from A.

percentage of inhibition occurred at a mole ratio of about 0.12 mol of compound per mole of tubulin indicating that the compounds are stoichiometric or weakly substoichiometric inhibitors of microtubule polymerization. Compound **1b** was considerably less active than the other three tested compounds showing only partial inhibition of microtubule assembly.

3.4. Cell based assays

The observed G₂/M arrest, coupled with the observed inhibition of microtubule assembly in vitro assays indicated that myoseverin, and its analogues **1a** and **1c**, may induce mitotic defects leading to mitotic arrest. Indeed, live cell imaging of HeLa cells expressing GFP-tubulin showed that addition of myoseverin (at 12 μM) in pre-assembled bipolar metaphase spindles led to the complete collapse of the spindle microtubules (Supplementary data, movie 1). Furthermore prometaphase cells were not capable of forming a normal bipolar spindle (Supplementary data, movie 2). In contrast, the interphase microtubule network was not visibly affected at similar conditions. (Supplementary data, movie 3). HeLa cells, exposed for 24 h at different concentrations of either myoseverin or analogues **1a** and **1c**, exhibited also a pronounced block at G₂/M similar to that presented in Table 2 (Fig. 3A). HeLa cells treated with myoseverin, **1a** and **1c**, were also observed by indirect immunofluorescence microscopy. At 12 μM, a concentration that led to strong G₂/M arrest (Fig. 3A), almost 100% of the mitotic spindles were aberrant, being monopolar or multipolar and in the rare occasions that a bipolar spindle was present not all of the chromosomes were aligned to the metaphase plate (Fig. 3B). A concentration dependent increase in the percentage of aberrant spindles in HeLa cells was also observed (Fig. 3C). Compound **1b** did not induce similar mitotic defects at concentrations as high as 50 μM.

4. Conclusion

Contrary to our previous work on CDK kinase analogue inhibitors,⁹ no improvement of the biological activity was observed when the purine nucleus was substituted by the pyrazolo[1,5-*a*]-1,3,5-triazine scaffold. Nevertheless, myoseverin derivatives **1a** and **1c** constitute a new series of tubulin inhibitors and displayed micromolar antiproliferative activities towards colorectal cancer cell lines. Compounds **1a** and **1c** can become new leads in the ongoing search of novel specific and potent anticancer drugs.

5. Experimental

5.1. General methods

Melting points were measured with a Büchi Tottoli SMP-20 heating unit and are uncorrected. IR spectra were recorded on a Perkin–Elmer 681 infrared spectrophotometer. NMR spectra were

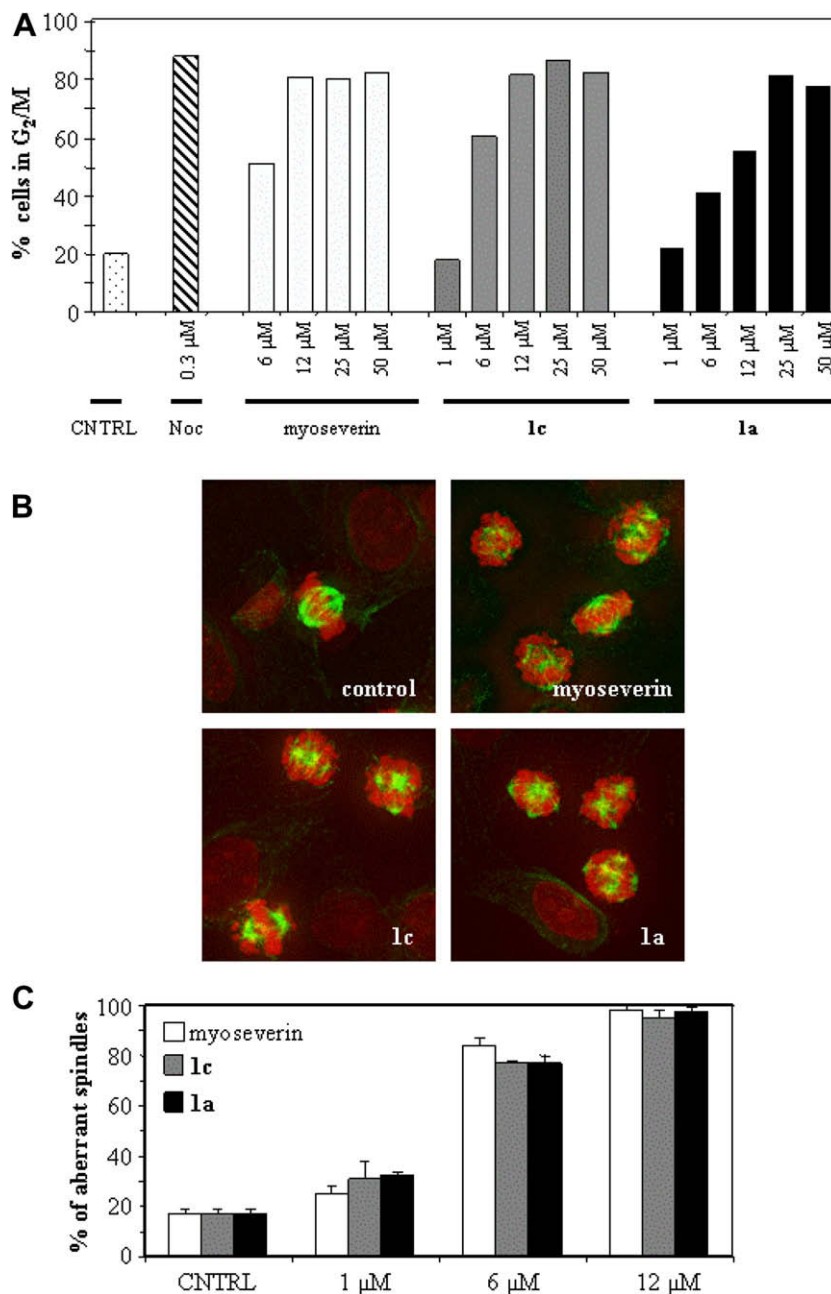


Figure 3. Induction of a mitotic block with aberrant spindles in the presence of myoseverin, and its analogues **1a** and **1c**, in HeLa cells. (A) HeLa cells were exposed to increasing concentrations of the inhibitors (myoseverin, **1a** and **1c**) for 24 h and the percentage of G₂/M cells was determined by flow cytometry. Nocodazole (Noc) was used as a control mitotic inhibitor. (B) Following addition of the drugs, cells were fixed and stained for indirect immunofluorescence microscopy (anti-tubulin: green; chromatin: red). Representative spindles of treated cells at 12 μM inhibitor concentration are shown. Control (CNTRL) refers to absence of inhibitor. (C) The percentages of aberrant spindles out of total spindles counted were determined for the different concentrations of each drug added.

recorded at 300 K on a Bruker Avance spectrometer at 300 MHz for ¹H and 75 MHz for ¹³C. Tetramethylsilane (TMS) was used as internal reference. Chemical shifts are expressed in parts per million (ppm) relative to TMS. It should be noted that quaternary carbon peaks of pyrazolo[1,5-*a*]-1,3,5-triazine ring of final compounds **1a**, **1b** and **1c** are not observed, these ¹³C NMR spectra are not reported in the experimental part. Mass spectra were recorded with a Perkin-Elmer SCIEX API spectrometer and Thermo Finnigan Mat 95 XL. Elemental analyses were performed on a Thermoquest Flash 1112 series EA analyser. TLC was conducted on precoated silica gel plates (Merck 60F₂₅₄) and the spots were visualized under UV light. Flash chromatography was carried out on a column filled with flash silica gel 60 (40–63 μm, Merck) using the indicated solvents

(petroleum ether (PE): bp 40–60 °C). All reactions requiring anhydrous conditions were conducted in flame-dried apparatus.

5.2. 4-(*N*-Methyl-*N*-phenylamino)-2-(methylsulfonyl)pyrazolo[1,5-*a*]-1,3,5-triazine (**3**)

Under inert atmosphere, 50% *m*-CPBA (656 mg, 1.90 mmol) was added to a solution of 4-(*N*-methyl-*N*-phenylamino)-2-(methylsulfonyl)pyrazolo[1,5-*a*]-1,3,5-triazine **2**¹⁰ (172 mg, 0.63 mmol) in CH₂Cl₂ (10 mL) at 0 °C. The reaction mixture was stirred at 0 °C for 1 h and was allowed to warm up to room temperature for 2 h. The reaction mixture was diluted by addition of CH₂Cl₂ (5 mL). The solution was washed with saturated aqueous solution

of NaHCO₃ (10 mL), then water (10 mL). The organic phase was dried over MgSO₄, then evaporated. The crude residue was purified by flash chromatography (EtOAc/PE 4:6) to afford compound **3** as a solid (150 mg, 78%). Mp = 174–175 °C (EtOH); IR (KBr) ν 3130, 2930, 2850, 1605, 1565, 1450, 1310, 930, 780 cm⁻¹; ¹H NMR (CDCl₃) δ 3.31 (s, 3H, CH₃), 3.88 (s, 3H, CH₃), 6.57 (d, 1H, *J* = 2.0 Hz, H₈), 7.22–7.25 (m, 2H, H_{arom}), 7.42–7.45 (m, 3H, H_{arom}), 7.83 (d, 1H, *J* = 2.0 Hz, H₇); ¹³C NMR (CDCl₃) δ 39.0 (CH₃), 43.1 (CH₃), 98.4 (CH), 126.4 (2 CH), 128.2 (CH), 129.3 (2 CH), 143.7 (C), 146.1 (CH), 149.8 (C), 150.4 (C), 159.5 (C); MS (ESI) *m/z* 304 (M+H)⁺; Anal. Calcd for C₁₃H₁₃N₅O₂S: C, 51.47; H, 4.32; N, 23.09. Found: C, 51.23; H, 4.18; N, 22.89.

5.3. N₂,N₄-Bis-(4-methoxybenzyl)pyrazolo[1,5-*a*]-1,3,5-triazine-2,4-diamine (**1a**)

In a sealed tube, a solution of compound **3** (120 mg, 0.38 mmol) and 4-methoxybenzylamine (209 μ L, 1.91 mmol) in dry dioxane (1 mL) was heated at 140 °C for 20 h. After cooling, the solvent was evaporated. The crude product was purified by flash chromatography (EtOAc/PE 3:7 then 4:6) to afford compound **1a** as a solid (101 mg, 70%). Mp = 144–146 °C (MeOH); IR (KBr) ν 3245, 2995, 1640, 1570, 1430, 1250, 1175, 765 cm⁻¹; ¹H NMR (CDCl₃) δ 3.80 (s, 6H, CH₃), 4.58 (d, 2H, *J* = 5.6 Hz, CH₂), 4.64 (d, 2H, *J* = 6.0 Hz, CH₂), 5.20 (br s, 1H, NH), 5.94 (br s, 1H, H₈), 6.62 (br s, 1H, NH), 6.85–6.88 (m, 4H, H_{arom}), 7.25–7.30 (m, 4H, H_{arom}), 7.73 (br s, 1H, H₇); MS (ESI) *m/z* 391 (M+H)⁺; Anal. Calcd for C₂₁H₂₂N₆O₂: C, 64.60; H, 5.68; N, 21.52. Found: C, 64.55; H, 5.79; N, 21.46.

5.4. 8-Bromo-4-(*N*-methyl-*N*-phenylamino)-2-(methylsulfonyl)pyrazolo[1,5-*a*]-1,3,5-triazine (**4**)

A solution of **2** (200 mg, 0.74 mmol) and *N*-bromosuccinimide (184 mg, 1.04 mmol) in dry CHCl₃ (20 mL) was stirred at reflux for 3 h. After evaporation of the solvent, the crude product was purified by flash chromatography (EtOAc/PE 1:9) to afford derivative **2** (104 mg, 82%) as a solid. Mp = 154–156 °C (EtOAc) IR (KBr) ν 3095, 2920, 1610, 1540, 760, 695 cm⁻¹; ¹H NMR (CDCl₃) δ 2.58 (s, 3H, CH₃), 3.71 (s, 3H, CH₃), 7.16 (d, 2H, *J* = 7.1 Hz, H_{arom}), 7.37–7.39 (m, 3H, H_{arom}), 7.56 (s, 1H, H₇); ¹³C NMR (CDCl₃) δ 14.4 (CH₃), 42.6 (CH₃), 81.1 (C), 126.2 (2 CH), 127.6 (CH), 129.2 (2 CH), 144.3 (CH), 145.0 (C), 147.8 (C), 147.9 (C), 168.3 (C); MS (ESI) *m/z* 350 (⁷⁹Br, M+H)⁺, 352 (⁸¹Br, M+H)⁺; Anal. Calcd for C₁₃H₁₂BrN₅S: C, 44.58; H, 3.45; N, 20.00. Found: C, 44.83; H, 3.62; N, 19.97.

5.5. 8-Bromo-4-(*N*-methyl-*N*-phenylamino)-2-(methylsulfonyl)pyrazolo[1,5-*a*]-1,3,5-triazine (**5**)

Following the procedure described for the preparation of **3**, compound **5** was obtained in 84% yield from **4** (132 mg, 0.38 mmol) and *m*-CPBA (1.13 mmol) in CH₂Cl₂ (6 mL). Chromatography eluent: EtOAc/PE 2:3. Mp = 195–197 °C (CH₂Cl₂/PE); IR (KBr) ν 3030, 2930, 2850, 1610, 1565, 1140, 745, 695 cm⁻¹; ¹H NMR (CDCl₃) δ 3.37 (s, 3H, CH₃), 3.82 (s, 3H, CH₃), 7.19–7.22 (m, 2H, H_{arom}), 7.40–7.45 (m, 3H, H_{arom}), 7.76 (s, 1H, H₇); ¹³C NMR (CDCl₃) δ 39.1 (CH₃), 43.6 (CH₃), 87.3 (C), 126.7 (2 CH), 128.6 (CH), 129.6 (2 CH), 143.6 (C), 146.4 (C), 146.9 (CH), 150.3 (C), 160.7 (C); MS (ESI) *m/z* 382 (⁷⁹Br, M+H)⁺, 384 (⁸¹Br, M+H)⁺; Anal. Calcd for C₁₃H₁₂BrN₅O₂S: C, 40.85; H, 3.16; N, 18.32. Found: C, 40.87; H, 3.08; N, 18.44.

5.6. 8-Bromo-N₂,N₄-bis-(4-methoxybenzylamino)pyrazolo[1,5-*a*]-1,3,5-triazine (**1b**)

Following the procedure described for the preparation of **1a**, compound **1b** was obtained in 70% yield from **5** (110 mg,

0.29 mmol) and 4-methoxybenzylamine (1.43 mmol) in dry dioxane (1.5 mL). Chromatography eluent: EtOAc/PE 3:7. Mp = 136–138 °C (MeOH washing); IR (KBr) ν 3245, 2925, 1640, 1580, 1430, 1245, 1175, 765 cm⁻¹; ¹H NMR (CDCl₃) δ 3.79 (s, 6H, 2 CH₃), 4.60 (s, 2H, CH₂), 4.62 (s, 2H, CH₂), 5.60 (br s, 1H, NH), 6.62 (br s, 1H, NH), 6.84–6.86 (m, 4H, H_{arom}), 7.21–7.24 (m, 4H, H_{arom}), 7.69 (s, 1H, H₇); MS (ESI) *m/z* 469 (⁷⁹Br, M+H)⁺, 471 (⁸¹Br, M+H)⁺; Anal. Calcd for C₂₁H₂₁BrN₆O₂: C, 53.74; H, 4.51; N, 17.91. Found: C, 53.80; H, 4.44; N, 18.14.

5.7. 8-(1-Methylethyl)-4-(*N*-methyl-*N*-phenylamino)-2-(methylsulfonyl)pyrazolo[1,5-*a*]-1,3,5-triazine (**7**)

A solution of 3 M methylmagnesium bromide in Et₂O (297 μ L, 2.58 mmol) was added dropwise to a solution of 8-acetyl-4-(*N*-methyl-*N*-phenylamino)-2-(methylsulfonyl)pyrazolo[1,5-*a*]-1,3,5-triazine **6**¹⁰ (269 mg, 0.86 mmol) in dry Et₂O (7 mL) cooled to 0 °C. After addition, the solution was stirred at room temperature for an additional 20 min. The reaction mixture was neutralized by a freshly prepared aqueous solution of NH₄Cl (5 mL). The aqueous layer was extracted with CH₂Cl₂ (5 mL) then EtOAc (2 \times 5 mL). The combined organic extracts were dried over MgSO₄ and concentrated. The oily residue was used without further purification. Under nitrogen atmosphere, a solution of the tertiary alcohol intermediate in CH₂Cl₂ (9 mL) was added at 0 °C to a solution of NaBH₄ (113.5 mg, 3.00 mmol) in TFA (9 mL). The reaction mixture was stirred at room temperature for 1 h and then neutralized by a solution of 1 M NaOH (15 mL). The aqueous layer was extracted with CH₂Cl₂ (3 \times 10 mL). The combined organic extracts were dried over MgSO₄ and evaporated. The residue was purified by flash chromatography (Et₂O/PE 1:9) to afford **7** (241 mg, 89%) as a solid. Mp = 85–87 °C (Et₂O/PE); IR (KBr) ν 3055, 2960, 2865, 1615, 1535, 1460, 750, 695 cm⁻¹; ¹H NMR (CDCl₃) δ 1.27 (d, 6H, *J* = 6.8 Hz, CH₃), 2.55 (s, 3H, CH₃), 3.14 (hept, 1H, *J* = 6.8 Hz, CH), 3.70 (s, 3H, CH₃), 7.15–7.19 (m, 2H, H_{arom}), 7.31–7.41 (m, 3H, H_{arom}), 7.54 (s, 1H, H₇); ¹³C NMR (CDCl₃) δ 14.3 (CH₃), 23.2 (2 CH₃), 23.5 (CH), 42.2 (CH₃), 113.9 (C), 126.2 (2 CH), 127.1 (CH), 129.1 (2 CH), 143.4 (CH), 144.9 (C), 147.4 (C), 148.4 (C), 164.9 (C); MS (ESI) *m/z* 314 (M+H)⁺; Anal. Calcd for C₁₆H₁₉N₅S: C, 61.32; H, 6.11; N, 22.34. Found: C, 60.99; H, 5.95; N, 22.36.

5.8. 8-(1-Methylethyl)-4-(*N*-methyl-*N*-phenylamino)-2-(methylsulfonyl)pyrazolo[1,5-*a*]-1,3,5-triazine (**8**)

Following the procedure described for the preparation of **3**, compound **8** was obtained in 65% yield from **7** (140 mg, 0.45 mmol) and *m*-CPBA (1.34 mmol) in CH₂Cl₂ (8 mL). Chromatography eluent: EtOAc/PE 1:2. Mp = 144–146 °C (EtOAc/PE); IR (KBr) ν 2960, 2870, 1600, 1555, 1460, 1045, 755, 705 cm⁻¹; ¹H NMR (CDCl₃) δ 1.27 (d, 6H, *J* = 6.8 Hz, CH₃), 3.21 (hept, 1H, *J* = 6.8 Hz, CH), 3.33 (s, 3H, CH₃), 3.83 (s, 3H, CH₃), 7.19–7.22 (m, 2H, H_{arom}), 7.39–7.42 (m, 3H, H_{arom}), 7.69 (s, 1H, H₇); ¹³C NMR (CDCl₃) δ 23.2 (2 CH₃), 23.5 (CH), 38.8 (CH₃), 42.9 (CH₃), 119.2 (C), 126.5 (2 CH), 128.0 (CH), 129.1 (2 CH), 143.9 (C), 144.5 (CH), 145.5 (C), 150.1 (C), 158.2 (C); MS (ESI) *m/z* 346 (M+H)⁺; Anal. Calcd for C₁₆H₁₉N₅O₂S: C, 55.64; H, 5.54; N, 20.27. Found: C, 55.88; H, 5.71; N, 20.39.

5.9. N₂,N₄-Bis-(4-methoxybenzylamine)-8-(1-methylethyl)pyrazolo[1,5-*a*]-1,3,5-triazine (**1c**)

Following the procedure described for the preparation of **1a**, compound **1c** was obtained in 79% yield from **7** (70 mg, 0.20 mmol) and 4-methoxybenzylamine (1.01 mmol) in dry dioxane (1 mL). Chromatography eluent: EtOAc/PE 1:4 then 1:2. Mp = 96–98 °C (EtOAc/PE); IR (KBr) ν 3285, 2955, 2865, 1635, 1555, 1445, 1250,

1175, 810 cm^{-1} ; $^1\text{H NMR}$ (CDCl_3) δ 1.30 (d, 6H, $J = 6.8$ Hz, CH_3), 3.06 (hept, 1H, $J = 6.8$ Hz, CH), 3.78 (s, 3H, CH_3), 3.79 (s, 3H, CH_3), 4.47 (s, 2H, CH_2), 4.49 (s, 2H, CH_2), 5.49 (br s, 1H, NH), 6.81 (d, 2H, $J = 8.3$ Hz, H_{arom}), 6.85 (d, 2H, $J = 8.5$ Hz, H_{arom}), 6.95 (br s, 1H, NH), 7.17 (d, 2H, $J = 8.3$ Hz, H_{arom}), 7.29 (d, 2H, $J = 8.5$ Hz, H_{arom}), 7.58 (br s, 1H, H_7); MS (ESI) m/z 433 ($\text{M}+\text{H}^+$); Anal. Calcd for $\text{C}_{24}\text{H}_{28}\text{N}_6\text{O}_2$: C, 66.65; H, 6.53; N, 19.43. Found: C, 66.88; H, 6.44; N, 19.49.

5.10. Cell lines

All cell lines were grown on 25 cm^2 flasks and were placed at 37 °C in a humidified atmosphere containing 5% CO_2 . The MCF-7 breast cancer cell line and the HCT116, SW48 and SW480 colorectal cancer cell lines were cultured in D-MEM culture medium containing 10% fetal calf serum, 1% L-glutamine and 2% penicillin-streptomycin. The Mes-sa sarcoma cell line and the CEM lymphoma cell line were cultured in RPMI1640 medium containing 10% fetal calf serum, 1% L-glutamine and 1% penicillin-streptomycin.

5.11. Cell growth inhibition assay

In vitro antiproliferative activities were determined in three separate experiments, each of which was performed in triplicate as previously described.¹¹ Briefly, asynchronously growing cells were transferred into 96-well culture plates (Costar[®], Corning Inc., New York) in 100 μL of medium at a final concentration of 5×10^3 cells/well and incubated for 24 h. Corresponding drug concentrations were then added to each plate. After 72 h of drug exposure, 20 μL of 3-[4,5-dimethylthiazol-2-yl]-2,5-diphenyltetrazolium bromide (MTT) reagent (5 mg/mL) was added to each well. Cell growth was expressed as the percent of absorbance of treated wells relative to untreated control wells. IC_{50} values were defined as drug doses resulting in 50% cell growth inhibition relative to untreated cells.

5.12. Flow cytometric detection of cell cycle (or cell cycle assay)

For analysis of DNA content and cell cycle distribution, colorectal cancer cell lines were treated with compounds **1a**, **1b**, **1c**, and myoseverin for 24 h. Based on cytotoxicity assay, a concentration of 30 μM (approx. IC_{80} values for these cell lines) was chosen for drug exposure experiments. After drug-exposure, 10^6 cells/mL were resuspended in 2 mL of propidium iodide solution (50 μL /mL), incubated at 4 °C overnight and then analyzed by flow cytometry. Flow cytometry was performed on a FACScalibur (Becton Dickinson, San Jose, California). Cell cycle distribution and DNA ploidy status were calculated after exclusion of cell doublets and aggregates on a FL2-area/FL2-width dot plot using Modfit LT 2.0[™] software (Verity Software Inc. Topsham, ME).

5.13. Microtubule polymerization assays

Microtubule polymerization assays in the absence or presence of inhibitors were performed in 96-well half-area μclear plates using a 96-well photometer (TECAN) measured at a wavelength of 340 nm. Tubulin was prepared as previously described.¹² Experiments were performed at the same time using the same buffers and tubulin from the same preparation to minimize variations originating from different experimental conditions. The final test volume was 50 μL prepared from solutions kept at 4 °C. To 33 μL PEM buffer (100 mM PIPES, 1 mM MgCl_2 , 1 mM EGTA), supplemented with increasing inhibitor concentrations in DMSO, tubulin at 12 mg/mL (29 μM) in PEM buffer was added, and carefully mixed. The polymerization into microtubules was followed at 340 nm over at least 1 h at 37 °C. The DMSO concentration was adjusted to be identical in all wells.

5.14. Live cell imaging and video microscopy

For time-lapse microscopy, HeLa cells expressing GFP-tubulin were plated in glass-bottom dishes then placed inside a video microscopy platform equipped with an incubator enabling the regulation of the temperature. The cell growth medium was replaced with the CO_2 independent growth medium DMEM/F12 with 15 mM HEPES (GIBCO) supplemented with 10% serum. Time-lapse Z series images ($Z = 3$) were collected with an inverted motorized microscope. Images were acquired with an inverted Olympus IX81 epifluorescence motorized microscope equipped with a motorized piezo stage (Ludl Electronic Products, USA) and a Retiga-SRV CCD camera (QImaging) driven by VOLOCITY software (Improvision) with a binning of 1, using a PlanApo 60xNA 1.42 objective (Olympus). Images were acquired every 5 min and the acquisition time was 53 ms. For each Z series, the best focus images was chosen before the reconstitution of the movie.

5.15. Immunofluorescence microscopy

HeLa cells were grown on Dulbecco's modified Eagle's medium (GIBCO, BRL) supplemented with 10% fetal bovine serum (Hyclone) and maintained in a humid incubator at 37 °C in 5% CO_2 . Cells were seeded and left to adhere for at least 36 h on poly-D-lysine-coated glass coverslips in 24 well plates. Drugs were diluted appropriately in medium from 50 mM stocks in 100% DMSO, and then added to the cells. Following 6 h incubation with drugs, cells were fixed with 1% paraformaldehyde-PBS at 37 °C for 3 min followed by 5 min incubation in 100% methanol at -20 °C. Coverslips were then washed with PBS and cells were stained with an anti- β -tubulin monoclonal antibody (Sigma) at 300-fold dilution for 1 h, then with an FITC-conjugated goat anti-mouse secondary antibody (Jackson ImmunoResearch Laboratories, West Grove, PA USA) at 250-fold dilution for 30 min and counterstained with propidium iodide. Images were acquired with an Olympus BX61 epifluorescence microscope equipped with a Retiga-SRV CCD camera driven by VOLOCITY software (Improvision).

Acknowledgments

We thank Rose-Laure Indorato for excellent technical assistance. We are grateful for financial support from the Association pour la Recherche sur le Cancer (ARC), grant number 3973.

Supplementary data

Supplementary data associated with this article can be found, in the online version, at [doi:10.1016/j.bmc.2009.03.007](https://doi.org/10.1016/j.bmc.2009.03.007).

References and notes

- (a) Rosania, G. R.; Chang, Y.-T.; Perez, O.; Sutherland, D.; Dong, H.; Lockhart, D.; Schultz, P. G. *Nat. Biotechnol.* **2000**, *18*, 304; (b) Chang, Y.-T.; Wignall, S. M.; Rosania, G. R.; Gray, N. S.; Hanson, S. R.; Su, A. I.; Merlie, J., Jr.; Moon, H.-S.; Sangankar, S. B.; Perez, O.; Heald, R.; Schultz, P. J. *Med. Chem.* **2001**, *44*, 4497; (c) Dvorák, Z.; Modrianský, M.; Vrba, J.; Ulrichová, J.; Krystof, V.; Stýskala, J.; Pávek, P. *Gen. Physiol. Biophys.* **2007**, *26*, 173.
- (a) Perez, O. M.; Chang, Y.-T.; Rosania, G.; Sutherland, D.; Schultz, P. G. *Chem. Biol.* **2002**, *9*, 475; (b) Duckmanton, A.; Kumar, A.; Chang, Y.-T.; Brockes, J. P. A. *Chem. Biol.* **2005**, *12*, 1117; (c) Ng, D. C. H.; Gebiski, B. L.; Grounds, M. D.; Bogoyevitch, M. A. *Cell. Motil. Cytoskel.* **2008**, *65*, 40.
- Park, H.-E.; Baek, S. H.; Min, J.; Chang, Y.-T.; Kang, D.-K.; Chang, S.-I.; Joe, Y. A. *DNA Cell Biol.* **2006**, *25*, 514.
- Hocek, M.; Votruba, I.; Dvorakova, H. *Tetrahedron* **2003**, *59*, 607.
- Krystof, V.; Moravcova, D.; Paprskarova, M.; Barbier, P.; Peyrot, V.; Hlobilkova, A.; Havlicek, L.; Strnad, M. *Eur. J. Med. Chem.* **2006**, *41*, 1405.
- Moon, H.-S.; Jacobson, E. M.; Khersonsky, S. M.; Luzung, M. R.; Walsh, D. P.; Xiong, W.; Lee, J. W.; Parikh, P. B.; Lam, J. C.; Kang, T.-W.; Rosania, G. R.; Schier, A. F.; Chang, Y.-T. *J. Am. Chem. Soc.* **2002**, *124*, 11608.

7. Raboisson, P.; Schultz, D.; Muller, C.; Reimund, J.-M.; Pinna, G.; Mathieu, R.; Bernard, P.; Do, Q.-T.; Desjarlais, R. L.; Justiano, H.; Lugnier, C.; Bourguignon, J.-J. *Eur. J. Med. Chem.* **2008**, *43*, 816.
8. Raboisson, P.; Baurand, A.; Cazenave, J.-P.; Gachet, C.; Schultz, D.; Spiess, B.; Bourguignon, J.-J. *J. Org. Chem.* **2002**, *67*, 8063.
9. (a) Bettayeb, K.; Sallam, H.; Ferandin, Y.; Popowycz, F.; Fournet, G.; Hassan, M.; Echalié, A.; Bernard, P.; Endicott, J.; Joseph, B.; Meijer, L. *Mol. Cancer Ther.* **2008**, *7*, 2713; (b) Popowycz, F.; Fournet, G.; Schneider, C.; Bettayeb, K.; Ferandin, Y.; Lamigeon, C.; Tirado, O. M.; Mateo-Lozano, S.; Notario, V.; Colas, P.; Bernard, P.; Meijer, L.; Joseph, B. *J. Med. Chem.* **2009**, *52*, 655.
10. Popowycz, F.; Bernard, P.; Raboisson, P.; Joseph, B. *Synthesis* **2007**, 367.
11. Galmarini, C. M.; Clarke, M. L.; Falette, N.; Puisieux, A.; Mackey, J. R.; Dumontet, C. *Int. J. Cancer* **2002**, *97*, 439.
12. Williams, R. C., Jr.; Lee, J. C. *Methods Enzymol.* **1982**, *85*, 376.